

Higgs boson production via Double Pomeron Exchange at the LHC

M. Boonekamp*, A. De Roeck†, R. Peschanski‡ and C. Royon§

We study Higgs boson production via Double Pomeron Exchange allowing for the presence of Pomeron remnants. We estimate the number of events produced at the LHC collider, as a function of the Higgs boson mass and its decay channel. The model which successfully describes the high mass dijet spectrum observed at Tevatron (run I) is used to predict rates of events with tagged protons for the acceptance range of the CMS/Totem experiments. Sizeable cross-sections and encouraging event selection signals are found, demonstrating especially for smaller Higgs boson masses the importance to study the diffractive channels. Tagging of the Pomeron remnants can be exploited to achieve a good resolution on the Higgs boson mass for inclusive diffractive events, by optimizing an intermediary analysis between higher cross-sections of the fully *inclusive* mode (all Pomeron remnants) and cleaner signals of the *exclusive* mode (without Pomeron remnants).

1. Introduction. It has been suggested [1,2] that diffractive Higgs boson production via Double Pomeron Exchange (DPE) is an interesting channel to study the Higgs boson at hadron colliders. The lack of a solid QCD based framework for diffraction made a purely theoretical study difficult. Recently [3] however, the possibility of a better determination of the cross-sections and event rates was proposed, using a model allowing the joint description of Higgs boson production and of the observed high mass dijet production at the Tevatron (run I) [4], allowing to compare and normalize the predictions to the data using a (simplified) simulation of the detector. One important difference with previous (purely *exclusive*) estimates lies on the consideration of *inclusive* production $pp \rightarrow p + X + H + Y + p$, see Fig. 1, namely with particles accompanying the Higgs/dijet production in the central region. We will call X, Y the “Pomeron remnants” in the following. The presence of the Pomeron remnants is vital for the good description of the dijet mass spectrum as discussed in [3].

Further estimates using a different Pomeron model [5]-a gives different numbers, since important sources of uncertainties still remain, but confirm the viability of such processes for the LHC. Pioneering studies which will be possible in the near future at the Tevatron [3,6], on the evaluation of experimental possibilities using outgoing (anti)proton tagging, on the resolution achievable with missing mass methods and with information on the Pomeron remnants, can be used to pin down remaining theoretical uncertainties. It can upgrade diffractive production to a complementary tool for the analysis of the Higgs boson characteristics at the LHC.

Our aim is to give predictions for Higgs boson production at the LHC based on *inclusive* dijet production at colliders via DPE. Thus, we **i)** normalize the theoretical predictions to the observed dijet rate at the Tevatron ($p\bar{p}$ collisions with $\sqrt{s} = 1.8$ TeV), and assume the obtained normalization factor is also valid at the LHC (pp collisions at $\sqrt{s} = 14$ TeV), **ii)** obtain a prediction for the Higgs boson production cross-sections and event rates at the LHC and, **iii)** discuss how the experimental opportunities at the LHC can be used for precision measurements.

In section **2**, we use as a starting point our model [3] based on the extension to *inclusive* diffractive production of the Bialas-Landshoff *exclusive* model for Higgs boson and heavy flavor jet production [1]. We showed [3] that this is able to reproduce the observed distributions, in particular the dijet mass fraction spectrum, the normalization being fixed from experiment.

The main lesson of our study is that an interesting potential for the Higgs boson studies at the LHC can be expected in double proton tagged experiments. In section **3**, we derive the predicted number of events as a function of M_H , depending on experimental cuts and the Higgs decay channel, and in section **4** the potentialities for Higgs mass reconstruction.

2. Formulation. Let us introduce the formulae for *inclusive* Higgs boson and dijet production cross-sections via DPE [3]:

$$d\sigma_H^{incl} = C_H \left(\frac{x_1^g x_2^g s}{M_H^2} \right)^{2\epsilon} \delta \left(\xi_1 \xi_2 - \frac{M_H^2}{x_1^g x_2^g s} \right) \prod_{i=1,2} \left\{ G_P(x_i^g, \mu) dx_i^g d^2 v_i \frac{d\xi_i}{1-\xi_i} \xi_i^{\alpha' v_i^2} \exp(-2v_i^2 \lambda_H) \right\},$$

*CERN, CH-1211, Geneva 23, Switzerland and CEA/DSM/DAPNIA/SPP, CE-Saclay, F-91191 Gif-sur-Yvette Cedex, France

†CERN, CH-1211, Geneva 23, Switzerland

‡CEA/DSM/SPhT, Unité de recherche associée au CNRS, CE-Saclay, F-91191 Gif-sur-Yvette Cedex, France

§CEA/DSM/DAPNIA/SPP, CE-Saclay, F-91191 Gif-sur-Yvette Cedex, France and Texas U. at Arlington, USA

$$d\sigma_{JJ}^{incl} = C_{JJ} \left(\frac{x_1^g x_2^g s}{M_{JJ}^2} \right)^{2\epsilon} F_{JJ} \delta^{(2)} \left(\sum_{i=1,2} (v_i + k_i) \right) \prod_{i=1,2} \left\{ G_P(x_i^g, \mu) d\xi_i d\eta_i d^2v_i d^2k_i \xi_i^{\alpha'v_i^2} \exp(-2v_i^2 \lambda_{JJ}) \right\}, \quad (1)$$

where x_1^g, x_2^g define, on each side (see Fig.1), the fraction of the Pomeron's momentum carried by the gluons involved in the hard process and $G_P(x_{1,2}^g, \mu)$, is, up to a normalization, the gluon structure function in the Pomeron extracted [7] from HERA experiments; μ^2 is the hard scale (for simplicity kept fixed at 75GeV^2 , the highest value studied at HERA; we neglect the small [7] contribution of quark initiated processes in the Pomeron); η_1, η_2 are the rapidities of the two jets and are defined as a function of the other kinematical variables by

$$m_{T1}^f e^{\eta_1} + m_{T2}^f e^{\eta_2} = \xi_1 x_1^g; \quad m_{T1}^f e^{-\eta_1} + m_{T2}^f e^{-\eta_2} = \xi_2 x_2^g, \quad (2)$$

where $m_{T_i}^f$ are the transverse mass of the quark with flavor f .

The formulae (1) are written for a Higgs boson of mass M_H and two jets (of total mass M_{JJ}), respectively. The Pomeron trajectory is $\alpha(t) = 1 + \epsilon + \alpha' t$ ($\epsilon \sim .08, \alpha' \sim .25 \text{ GeV}^{-2}$), $\xi_{1,2}$ (< 0.1) are the Pomeron's fraction of longitudinal momentum, $v_{1,2}$, the 2-transverse momenta of the outgoing $p\bar{p}$, $k_{1,2}$ those of the outgoing quark jets, $\lambda_H \sim 2 \text{ GeV}^{-2}$ (resp. $\lambda_{JJ} \sim 3 \text{ GeV}^{-2}$) the slope of the non perturbative coupling for the Higgs boson (resp. dijets), and the constants C_H, C_{JJ} are normalizations including a non-perturbative gluon coupling [1], appreciably cancelled in the ratio C_H/C_{JJ} .

The dijet cross-section σ_{JJ} depends on the $gg \rightarrow \bar{Q}^f Q^f$ and $gg \rightarrow gg$ cross-sections [8]. This gives for five quark flavors

$$F_{JJ} = \sum_f F_{\bar{Q}^f Q^f}(\rho^f) + 54 F_{gg}(\rho^{gg}); \quad \rho^f \equiv \frac{4 m_{T1}^f m_{T2}^f}{M_{\bar{Q}^f Q^f}^2}; \quad \rho^{gg} \equiv \frac{4 p_{T1} p_{T2}}{M_{gg}^2},$$

$$F_{\bar{Q}^f Q^f} \equiv \frac{\rho^f}{m_{T1}^2 m_{T2}^2} \left(1 - \frac{\rho^f}{2} \right) \left(1 - \frac{9\rho^f}{16} \right); \quad F_{gg} \equiv \frac{1}{p_{T1}^2 p_{T2}^2} \left(1 - \frac{\rho^{gg}}{4} \right)^3. \quad (3)$$

The colour factor 54 appears in the ratio of gluon jets *vs.* quark jets partonic cross-sections [8].

Note that the $gg \rightarrow \bar{Q}^f Q^f$ cross section depend on *transverse* and not on *rest* quark masses. Thus, all 5 quark flavors sizeably contribute to the dijet cross-section. This is to be contrasted with the *exclusive* case which is proportional to *rest* masses [1,3], and thus considerably smaller.

The physical origin of formulae (1) is the following: since the overall partonic configuration is produced initially by the long-range, soft DPE interaction, we assume that, up to a normalization, the *inclusive* cross-section is the convolution of the "hard" *partons* \rightarrow *Higgs boson*, (or *partons* \rightarrow *jets*) subprocesses by the Pomeron structure function into gluons, see Fig.1. The expected factorization breaking of hadroproduction will appear in the normalization through a renormalization of the Pomeron fluxes, which are not the same as in hard diffraction at HERA. Indeed, this ansatz remarkably reproduces the dijet mass fraction seen in experiment, see Ref. [3]. This model has been successfully applied [3] to Tevatron data on dijets and to predictions for Higgs production possibilities at the same accelerator [3].

3. Predictions. We can now give predictions for the Higgs boson production cross sections in DPE events at the LHC, i.e. with $\xi_{1,2} < 0.1$, by scaling our results by the same factor used for the CDF measurement on dijet cross sections, which means increasing it by a factor 3.8 [3]. The results are given in Table 1 (first column) and in Fig. 2. We note the high values of the cross-sections. Since the typical luminosity for the LHC will be of the order of $10\text{-}100 \text{ fb}^{-1}/\text{year}$, this leads to several thousand Higgs particles diffractively produced per year, even at low luminosity. It is of course imperative to study the corresponding background, on which we will comment after final selection in section 4. Hence for the inclusive channel the cross section is large, much larger than recent calculations for the exclusive channel (see Ref. [5]-b). In Ref. [5]-a, similar conclusions are reached (note however [5]-c).

In Fig. 2, we show the effects of the acceptance of the possible roman pots detectors at the LHC, which are used in conjunction with a central detector. Following ideas presently discussed in a common study group of the central detector CMS [9] and the elastic/soft diffraction experiment TOTEM [10], which both will use the same interaction region at the LHC, we choose four possible configurations for roman pot detectors to measure the scattered protons. The used acceptance numbers are based on [11]. The first one (see, *Config.1* on Fig.2) has roman pot detectors located in the warm region of the LHC respectively at 140-180 meters and 240 meters and assumes a good acceptance for protons with $|t| < 2 \text{ GeV}^2$, and $\xi > 0.01$. The second one (*Config.2*) considers only roman pots at 140-180 meters [10] and gives a good acceptance only for $|t| < 1.5 \text{ GeV}^2$, and $\xi > 0.02$. *Config.3* assumes the presence of roman pot detectors in the cold region of the LHC at about 425 meters and gives a good acceptance for $|t| < 2 \text{ GeV}^2$, and $0.002 < \xi < 0.02$. Certainly the latter will be challenging both from the machine and experimental point of view, but Fig.2 demonstrates that such detectors are needed to obtain a good acceptance for low mass Higgs production.

Config.4 corresponds to the full system using all detectors. In Table 1, the acceptance of the roman pot detectors in the case of *Config.4* is taken into account, and we give the number of events for 10 fb^{-1} in the different Higgs decay modes.

4. Higgs boson mass reconstruction. The advantage of DPE events with respect to standard Higgs boson production lies in offering a potential to reconstruct the Higgs particle parameters more precisely. For example, one can hope to obtain a very precise Higgs mass reconstruction if one can tag and measure both the protons in the roman pot detectors as well as the Pomeron remnants.

In Fig. 3 (upper part), we show the distribution in pseudo-rapidity of the tagged proton (highest $|\eta|$), the Pomeron remnants at the parton level (medium $|\eta|$) and the Higgs decay products for a Higgs mass of 120 GeV in our model. In Fig. 3 we also give the size of the rapidity gap between the tagged proton and the Pomeron remnant in the case of a Higgs mass of 120 GeV (middle left), 700 GeV (middle right). In the last row of this figure we show the distance between the Pomeron remnant and the nearest jet from the Higgs, for the two Higgs masses. The rapidity distance is large at the parton level. This region will be however mostly filled with soft particles from QCD radiation and from hadronization of the partons. We nevertheless expect that the remnants will remain visible after a cut on soft activity¹ (e.g. particles below 1 GeV).

In Fig. 4, we describe the results of the Higgs boson mass reconstruction assuming one is able to select and measure the Pomeron remnants. Then the Higgs boson mass can be reconstructed by applying quadri-momentum conservation to all particles in the final state, namely the Higgs boson, the scattered protons in the roman pot detectors, and the Pomeron remnants. The energy $E = \sqrt{\xi_1 \xi_2 s}$ is used to produce the Higgs boson and the Pomeron remnants. Detecting these remnants requires the presence of detectors with an acceptance at high pseudo-rapidity, ideally up to $|\eta| = 10$ (see Fig. 3), but already taggers up to a rapidity of 7.5-8 [9] give a good acceptance for a Higgs boson with a mass of 120 GeV. With such taggers, it is possible to reconstruct Higgs boson masses² up to about 600 GeV.

The quality of the reconstruction of the remnants needs to be demonstrated after including hadronization and detector effects, and are subject to a future detailed study. Meanwhile we assume it can be done with a resolution of $100\%/\sqrt{E}$ (resp. $300\%/\sqrt{E}$) in an optimistic (resp. more pessimistic) scenario. The mass distribution is then determined from the missing mass measurement from the scattered protons, and the remnants are subtracted. The smearing on the resulting Higgs mass distribution is mainly due to the Pomeron remnant measurements, hence a good resolution can be obtained when the energy of the Pomeron remnants is small, *i.e.* a configuration nearer to the *exclusive* case.

In Fig. 4, we display the resolution (resp. 2.1, 4.0, 4.6 and 6.6 GeV) on the Higgs boson mass reconstruction for four different cuts on the Pomeron remnant energy (resp. 20, 50, 100 and 500 GeV) and for the optimistic scenario. This does not take into account the additional resolution smearing of 1-2 GeV expected from the missing mass analysis of the scattered protons [11]. The plot with the best resolution (2.1 GeV) is shown for a luminosity of 30 fb^{-1} . When the configuration is close to an *exclusive* process, *i.e.* the remnant energy is less than 20 GeV, this leads respectively to a resolution of 2.1, 3.6 and 4.7 GeV for a Higgs boson mass of 120, 200 and 500 GeV. In the more pessimistic scenario, the resulting Higgs mass resolution is about 7 GeV for a 120 GeV Higgs. A good coverage in pseudo-rapidity will be essential to be able to precisely measure the Higgs boson parameters. Note that the events showing little energy for the Pomeron remnants have a low value of ξ , since $M_H \sim \sqrt{\xi_1 \xi_2 s}$, which leads to $\xi_1 \xi_2 \sim 7 \cdot 10^{-5}$. Hence roman pot detectors in the region of about 400 m from the interaction point will be essential.

At the LHC it is also important to consider background events. While a full study is deferred to a follow up paper, we determined that the signal over background ratio is enhanced compared to the non diffractive case because of the good resolution on the dijet mass and the cut on the mass window. Initial studies indicate that the $b\bar{b}$ channel might be interesting to look for Higgs in the diffractive mode.

To summarize, we have shown that the diffractive inclusive Higgs production leads to large event rates at the LHC. A Higgs mass reconstruction with good precision is possible if both protons in the final state can be tagged with roman pot detectors and if the Pomeron remnants can be measured in the forward region with sufficient resolution. This channel and method will be especially useful in the low mass Higgs region where the standard methods for Higgs measurements at the LHC are challenging.

¹Such a cut may anyway be required in the analysis to reduce the effects of soft inelastic overlaid pile-up events due to multiple interactions per bunch crossing at the LHC.

²The precision obtained on the Higgs boson mass reconstruction using standard events is quite high for high Higgs boson masses. Our method is especially useful at low Higgs masses where the measurement is harder for standard events.

REFERENCES

- [1] A. Bialas and P.V. Landshoff, *Phys. Lett.* **B256** (1990) 540, A. Bialas and W. Szeremeta, *Phys. Lett.* **B296** (1992) 191, A. Bialas and R. Janik, *Zeit. für. Phys.* **C62** (1994) 487.
- [2] A. Schafer, O. Nachtmann and R. Schöpf, *Phys. Lett.* **B249** (1990) 331, J.D. Bjorken, *Phys.Rev.* **D47** (1993), J-R Cudell and O.F. Hernandez, *Nucl. Phys.* **B471** (1996) 471; H.J. Lu, J. Milana *Phys.Rev.* **D51** (1995) 6107; D. Graudenz, G. Veneziano *Phys. Lett.* **B365** (1996) 302; M. Heyssler, Z. Kunszt, W.J. Stirling, *Phys. Lett.* **B406** (1997) 95; E.M. Levin, hep-ph/9912403 and references therein; V.A. Khoze, A.D. Martin and M.G. Ryskin, *Eur.Phys.J.* **C14** (2000) 525, *id.* **C19** (2001) 477, hep-ph/0006005; V.A. Khoze, hep-ph/0105224.
- [3] M. Boonekamp, R. Peschanski and C. Royon, *Phys. Rev. Lett.* **87** (2001) 251806. Note that initial misprints have been corrected in formulae (1) and (3) of the present paper.
- [4] T. Affolder et al. , CDF Coll. , *Phys. Rev. Lett.* **85** (2000) 4215.
- [5] -a B. Cox, J. Forshaw, B. Heinemann, hep-ph/0110173;
 -b Similar conclusion but mainly for *exclusive* production: V.A. Khoze, A.D. Martin, M.G. Ryskin, hep-ph/0203122.
 -c Model using a different (non Pomeron) mechanism favoring single diffractive over DPE Higgs production at the LHC: R. Enberg, G. Ingelman, A. Kissavos, N. Timneanu, hep-ph/0203267.
- [6] M.G. Albrow and A. Rostovtsev, hep-ph/0009336.
- [7] C. Royon, L. Schoeffel, J.Bartels, H.Jung, R.Peschanski, *Phys. Rev.* **D63** (2001) 074004.
- [8] B.L. Combridge and C.J. Maxwell, *Nucl. Phys.* **B239** (1984) 429.
- [9] CMS Collab., Technical Design Report (1997).
- [10] TOTEM Collab., Technical Design Report, preprint CERN/LHCC 99-7.
- [11] R. Orava, talk at LISHEP02, Rio de Janeiro, February 2002.

TABLE

$M_{Higgsboson}$	(1)	(2)	(3)	(4)	(5)	(6)
120	3219	2043	228	447	48	0
150	2637	417	48	1827	222	0
200	1995	3	0	1470	522	0
300	1419	0	0	984	438	0
375	1674	0	0	1047	483	138
500	813	0	0	441	213	156
700	126	0	0	72	33	18
1000	4	0	0	2	1	0

TABLE I. *Number of Higgs boson events for $10 fb^{-1}$.* The first column gives the number of events at the generator level (all decay channels included), and the other columns take into account the roman pot acceptance and give the number of events for different Higgs boson decay channels (2: $b\bar{b}$, 3: $\tau^+\tau^-$, 4: WW , 5: ZZ , 6: $t\bar{t}$).

FIGURES

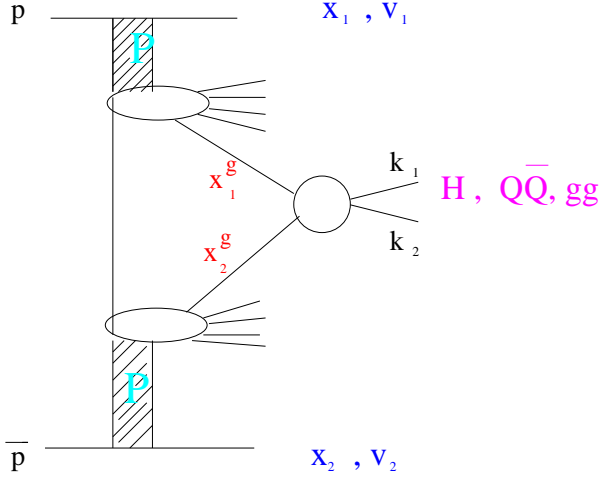


Figure 1

Production scheme.

$x_i \equiv 1 - \xi_i, v_i$ are the longitudinal and transverse 2-momenta of the diffracted (anti)proton (see formula (1) and text for the other kinematical notations).

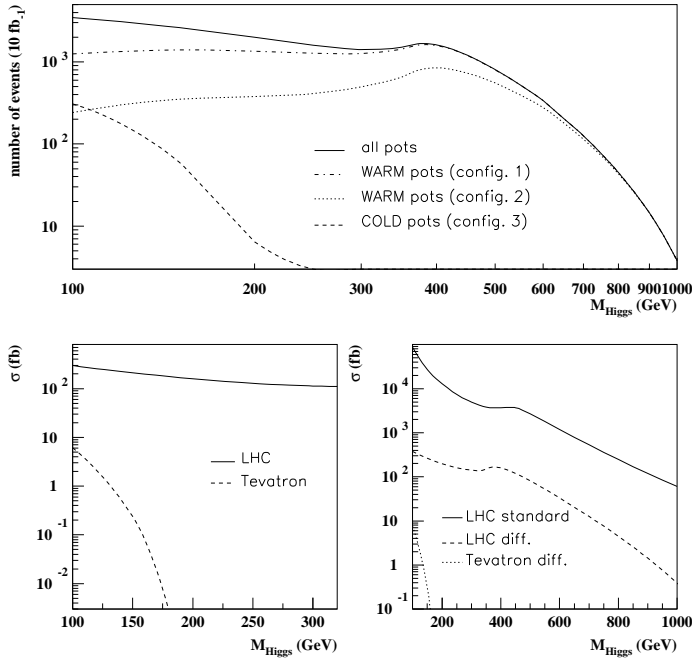


Figure 2

Diffractive Higgs boson production cross section

Upper plot: number of Higgs boson events for 10 fb^{-1} as a function of M_H obtained for different roman pot configurations (see text). *Bottom plots:* Diffractive Higgs boson production cross section as a function of M_H for the LHC (and the Tevatron). The standard inclusive Higgs boson production cross section is also shown for comparison.

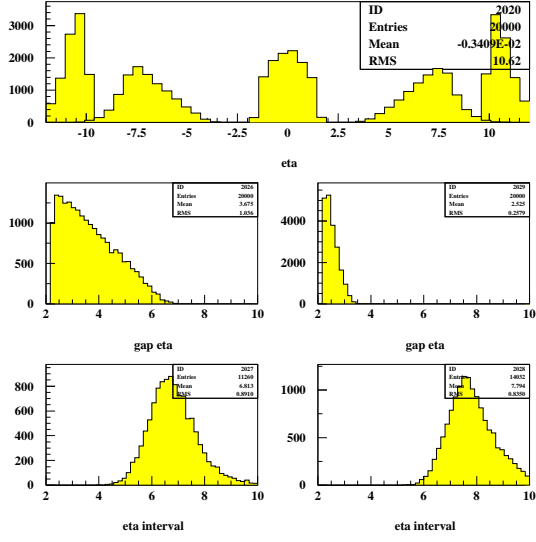


Figure 3

Pseudo-rapidity distributions

Upper plot: pseudo-rapidity distributions of the tagged protons, Pomeron remnants (parton level) and Higgs boson decay products for $M_H = 120\text{GeV}$; Medium plots from left to right: rapidity gap distribution between the tagged proton and the Pomeron remnant for two cases $M_H = 120\text{GeV}$, $M_H = 700\text{GeV}$; Bottom plots: Distance between the Pomeron remnant (parton level) and the nearest jet from the Higgs boson, for $M_H = 120\text{GeV}$, $M_H = 700\text{GeV}$.

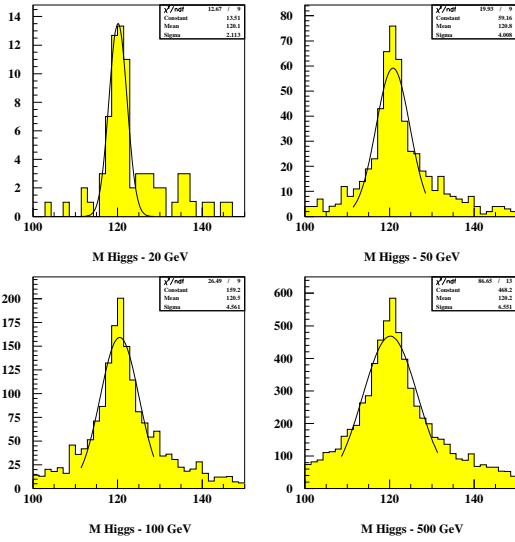


Figure 4

Higgs mass resolution

The resolution on the Higgs boson mass is shown after four different cuts on the Pomeron remnant energies at 20, 50, 100 and 500 GeV for a luminosity of 30fb^{-1} .